Thermochimica Acta, 209 (1992) 175–188
Elsevier Science Publishers B.V., Amsterdam

Kinetic compensation effect for the thermal solid state reactions of lanthanide oxalate, malonate and succinate hydrates and their anhydrides

Kazuo Muraishi
Department of Chemistry, Faculty of Science, Yamagata University, Yamagata 990 (Japan)

Hiroko Yokobayashi
College of General Education, Tohoku University, Kawauchi, Sendai 980 (Japan)
(Received 22 January 1992)

Abstract

The kinetic parameters of the thermal reactions of lanthanide oxalate, malonate and succinate hydrates and their anhydrides have been derived by means of the Coats and Redfern method on the basis of the TG runs. The kinetic compensation effect was observed between the activation energies (E_a) and the pre-exponential factors (A). The plots of E_a vs. $\lg A$, except for the decomposition of the succinates, showed two linear portions for the light and the heavy lanthanides as a reflection of the double periodicity between the former and latter half of the lanthanide sequence.

INTRODUCTION

The compensation effect is the synchronous variation of the pre-exponential factor (A) and the activation energy (E_a) of a reaction with a group of rate processes, and is one of the controversial fields of chemical research. The discussion of the compensation effect in heterogeneous catalysis has had a long history; it was found first by Constable [1] and described in detail by Cremer and Schwab [2]. It describes a linear relationship between $\lg A$ and E_a derived from the Arrhenius equation, and is often expressed as

$$\lg A = aE_a + b \tag{1}$$

where a and b are constants. This behaviour has been summarized by Galwey [3]. McCoy [4] supposed that when the molecule is adsorbed at a catalytically active site the bond can become more anharmonic. In this case, E_a and A decrease. McCoy has also described the compensation

Correspondence to: K. Muraishi, Department of Chemistry, Faculty of Science, Yamagata University, Yamagata 990, Japan.

effect due to vibrational relaxation processes, and the dissociation step in certain catalyzed reactions has been examined [4, 5]. Although a compensation behaviour between $\ln A$ and E_a has been widely reported in the literature. Agrawal [6] recommended that investigators wishing to establish the compensation effect should show a plot of $\ln k$ vs. inverse temperature instead of $\ln A$ vs. E_a, where k is the rate constant. This should aid in eliminating scepticism. It will also lead to a better understanding of the compensation effect. This effect is by no means limited to the phenomenon of heterogeneous catalysis, and has been observed in homogeneous processes [7].

Occurrence of such a compensating behaviour between $\lg A$ and E_a has been widely investigated in recent years. In particular, the existence of the compensation effect in the thermal dehydration and decomposition reactions of solid inorganic and organic materials has been reported: the dehydroxylation of kaolinite [8], the dehydration of $Ba(ClO_3)_2 \cdot H_2O$ [9] and $MgC_2O_4 \cdot 2H_2O$ [10], and the decomposition of NH_4ClO_4 [11], $(CH_3NH_3)_2MnCl_4$ [12], cellulosic materials [13], $CdCO_3$, $MnCO_3$ and $PbCO_3$ [14], butyl rubber [15], $LnCr(gluconate)_4 \cdot nH_2O$ (Ln = lanthanide) [16], and basic aluminium salts [17].

Research on this effect has also been carried out in various fields, for example, the selective oxidation reactions or propenes [18], the connections to linear free energy relationships [19], the photoadsorption kinetics of amorphous Se colloids [20], the conductivity of $BaTiO_3$ doped with Nb^{5+} under different partial pressures of O_2 at 1000°C [21], the viscosity–temperature dependence of polymer melts [22], the dehydrogenation of

TABLE 1

The classification of prepared oxalate, malonate and succinate hydrates by their hydration numbers (n)

Compound	Ln	n
Oxalates		
$Ln_2ox_3 \cdot nH_2O$	La–Ho	10
	Er	6
	Tm–Lu	5
Malonates		
$Ln_2mal_3 \cdot nH_2O$	La	5
	Ce–Eu	6
	Gd–Lu	8
Succinates		
$Lu_2suc_3 \cdot nH_2O$	La	6
	Ce–Ho	5
	Er	7
	Tm–Lu	5

Key: Ln, lanthanide; ox, oxalate; mal, malonate; suc, succinate.

ethylene in the presence of Pt/SiO_2 catalysts with different crystallite sizes [23], the theory of enthalpy–entropy compensation in ion exchange equilibrium [24], and the apparent linear relationship between E_a and $\lg A$ and between enthalpy and entropy [25].

So far, we have reported the thermal dehydration and decomposition of metal complexes of malonic acid [26a] and succinic acid [26b]. It is

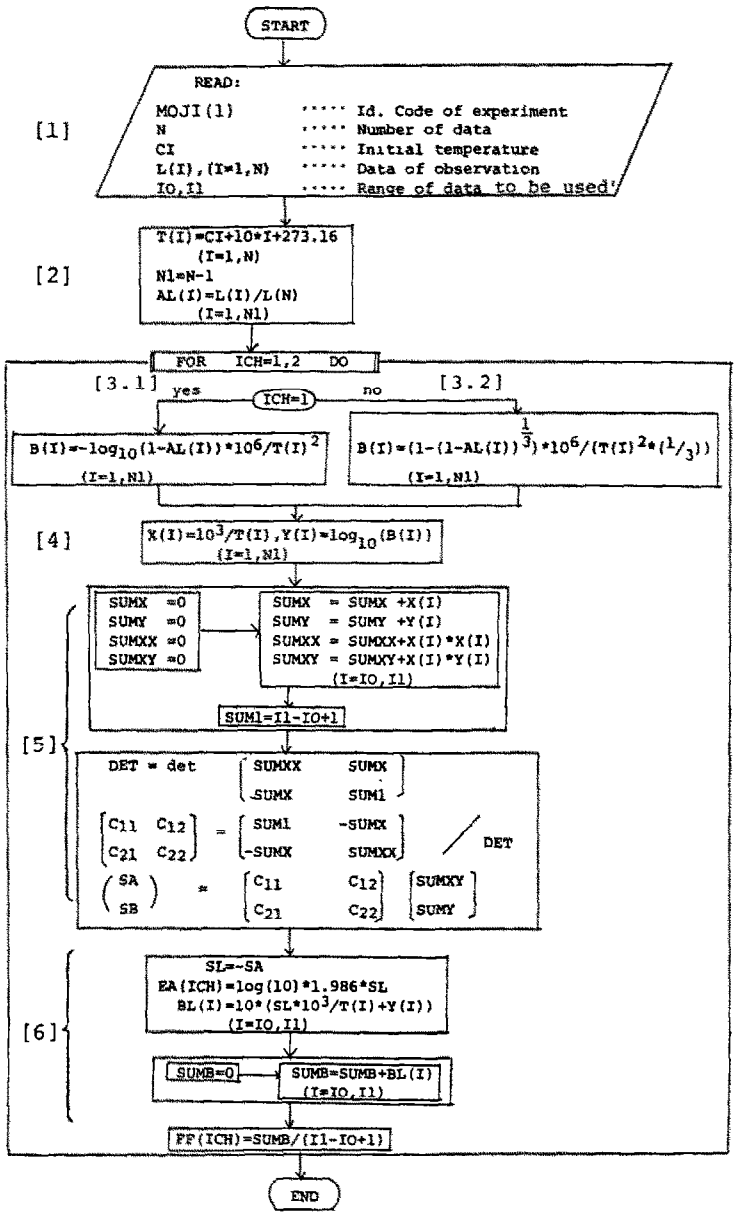

Fig. 1. Computer flow diagram for calculation of the activation energy (E_a) and frequency factor (A) by the least-squares method.

interesting to discover how the chemical character depending upon the presence or otherwise of a methylene group in the dicarboxylates reflects on the compensation effect. In this paper we shall attempt this and also highlight the importance of statistical analysis in respect of the kinetics of the thermal dehydration and decomposition of lanthanide oxalates, malonates, and succinates, with computer-aided treatment of thermogravimetric data, and we shall investigate whether conclusions can be drawn regarding the occurrence of compensation behaviour.

EXPERIMENTAL

Materials and measurements

The preparation of the lanthanide oxalate, malonate and succinate hydrates and the procedures of TG–DTA were described in the preceding paper [27]. The results of elemental analyses for C, H and metals agreed with the calculated values within approx. ±0.3%. From the results of elemental analyses and weight-loss values of the dehydration step, reasonable empirical formulae were found to be those shown in Table 1. The starting oxalate, malonate and succinate samples were classified from the differences in hydration number. The TG–DTA curves were simultaneously recorded with a Shinku Riko TGD-3000RH apparatus at a heating rate of 3 K min^{-1} in N_2 flowing at 30 ml min^{-1}.

Kinetic analysis of experimental data

Non-isothermal kinetics

The activation energies (E_a) and frequency factors (A) were calculated by using the Coats–Redfern method [28] applied to the TG curves. This method is one of the approximations widely employed as a reliable method [29]. This method allows a good linearization if the correct n value is assumed

$$\lg\left[\frac{1-(1-\alpha)^{1-n}}{T^2(1-n)}\right] = \lg\frac{AR}{\phi E_a}\left[1-\frac{2RT}{E_a}\right] - \frac{E_a}{2.3RT} \qquad (2)$$

where ϕ denotes the heating rate, α is the degree of reaction and n is the reaction order. A digital computer program has been written for the determination of E_a and A of the Arrhenius equation for the raw data obtained to accept the sample weight w and sample temperature T as a function of time t from the TG curves. The flow diagram for calculation of E_a and A is shown in Fig. 1 (see Appendix). All calculations were performed on an Okitak 50 digital computer using a FORTRAN IV program. Primary information was collected automatically with a programmable calculator, which in definite time intervals corresponding to a prescribed

temperature step takes a signal proportional to the sample weight from the TG apparatus. A subsequent routine allows the calculation of α values at selected temperatures. The computer program makes use of a least-squares polynomial fit of the time–sample weight values and calculates the reaction rate constant for any point chosen on the TG curve. The plot for the Coats–Redfern method gives straight lines whose slopes and intercepts yield E_a and A, respectively.

Isothermal kinetics

To ensure the validity of E_a values obtained by the Coats–Redfern method, the Ng method [30] was used, which allows the determination of kinetic parameters from a single isothermal kinetic run. There is a comprehensive table in which the most commonly used expressions for the kinetics of thermal decomposition are presented in terms of the general

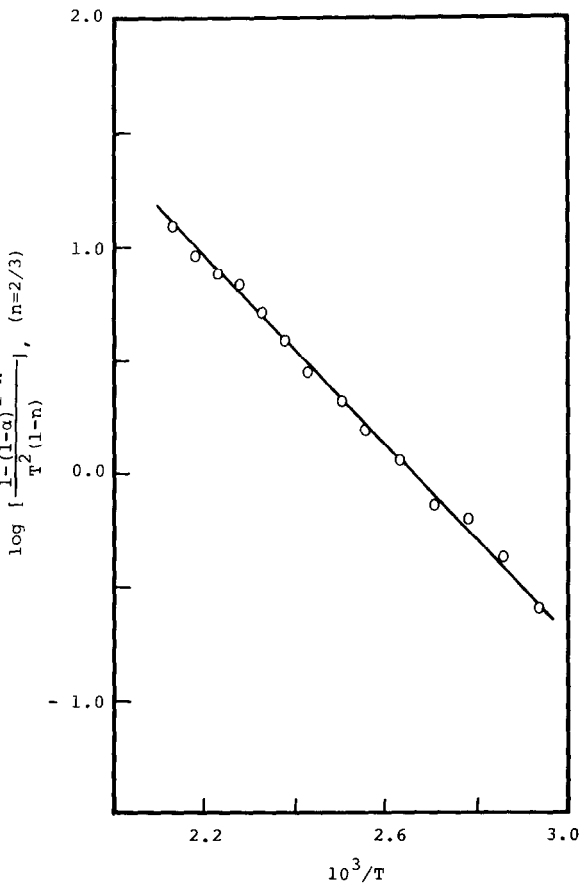

Fig. 2. Plot by the Coats–Redfern method for the dehydration process of samarium oxalate decahydrates $Sm_2ox_3 \cdot 10H_2O$ in a flowing N_2 atmosphere.

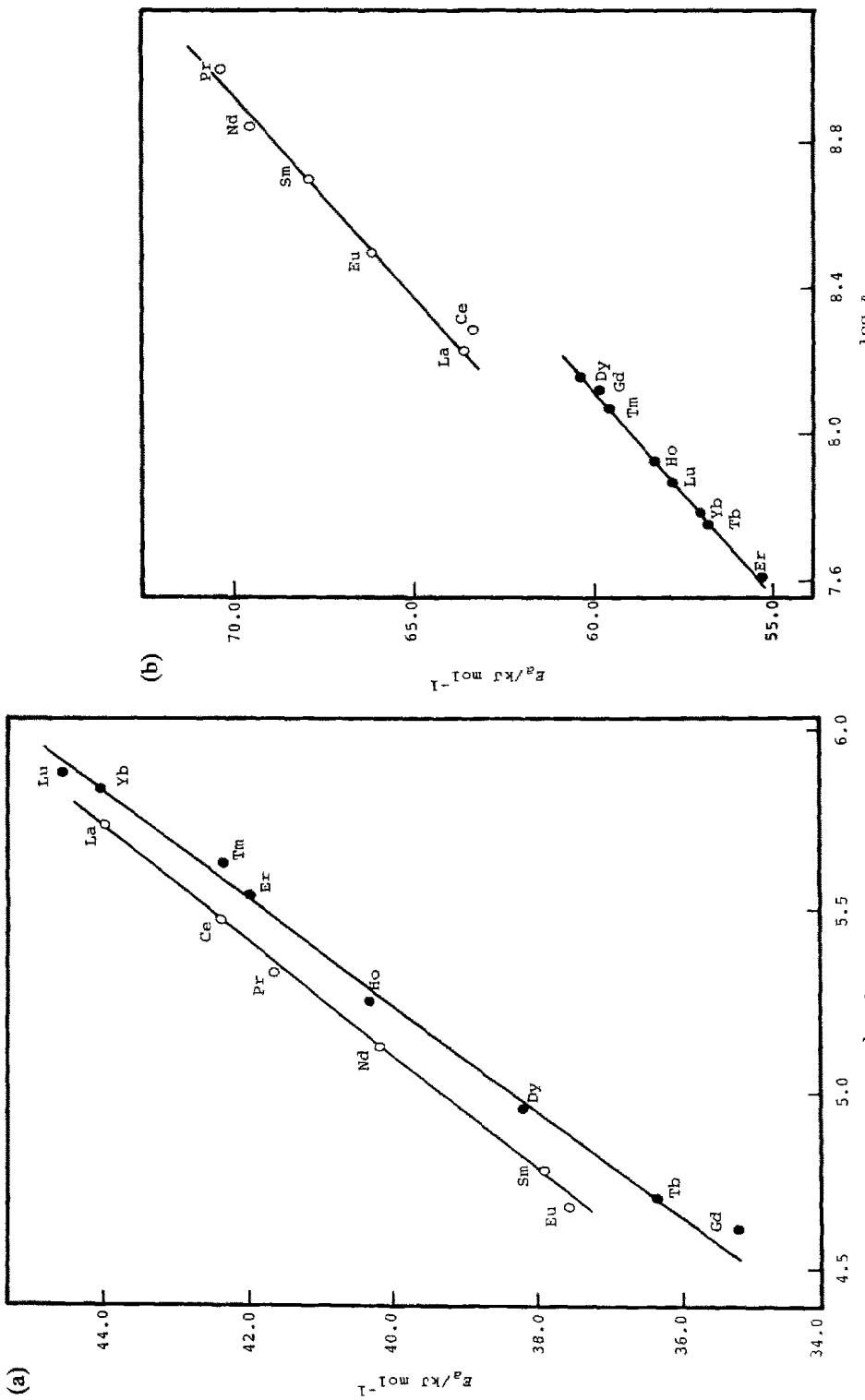

Fig. 3. Kinetic compensation effect in the thermal dehydration of (a) $Ln_2ox_3 \cdot nH_2O$, (b) $Ln_2mal_3 \cdot nH_2O$ and (c) $Ln_2suc_3 \cdot nH_2O$ in a flowing N_2 atmosphere. ○, light lanthanide; ●, heavy lanthanide.

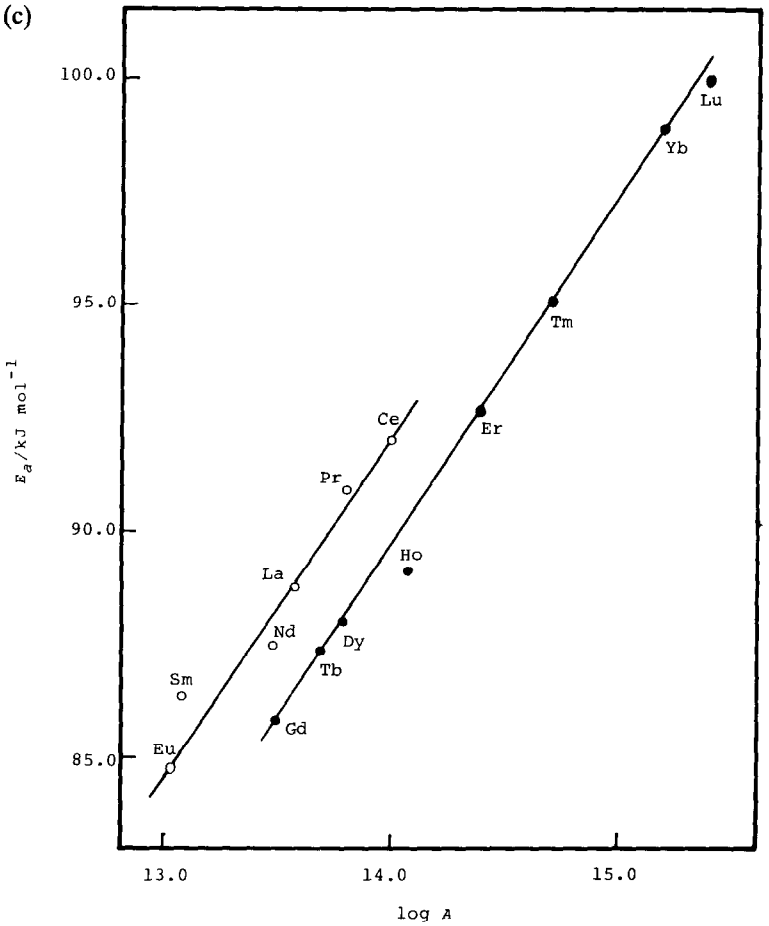

Fig. 3 (continued)

differential form

$$\frac{d\alpha}{dt} = k^{1-p}(1-\alpha)^{1-q} \tag{3}$$

where $0 \leqq p \leqq 1$ and $0 \leqq q \leqq 1$, and k is the rate constant given by the expression

$$k = A\, e^{-E_a/RT} \tag{4}$$

Combining eqns. (3) and (4)

$$\ln\left(\frac{d\alpha}{dt}\right)_T = -\frac{E_a}{RT} + \text{const} \tag{5}$$

where T is the temperature at time t.

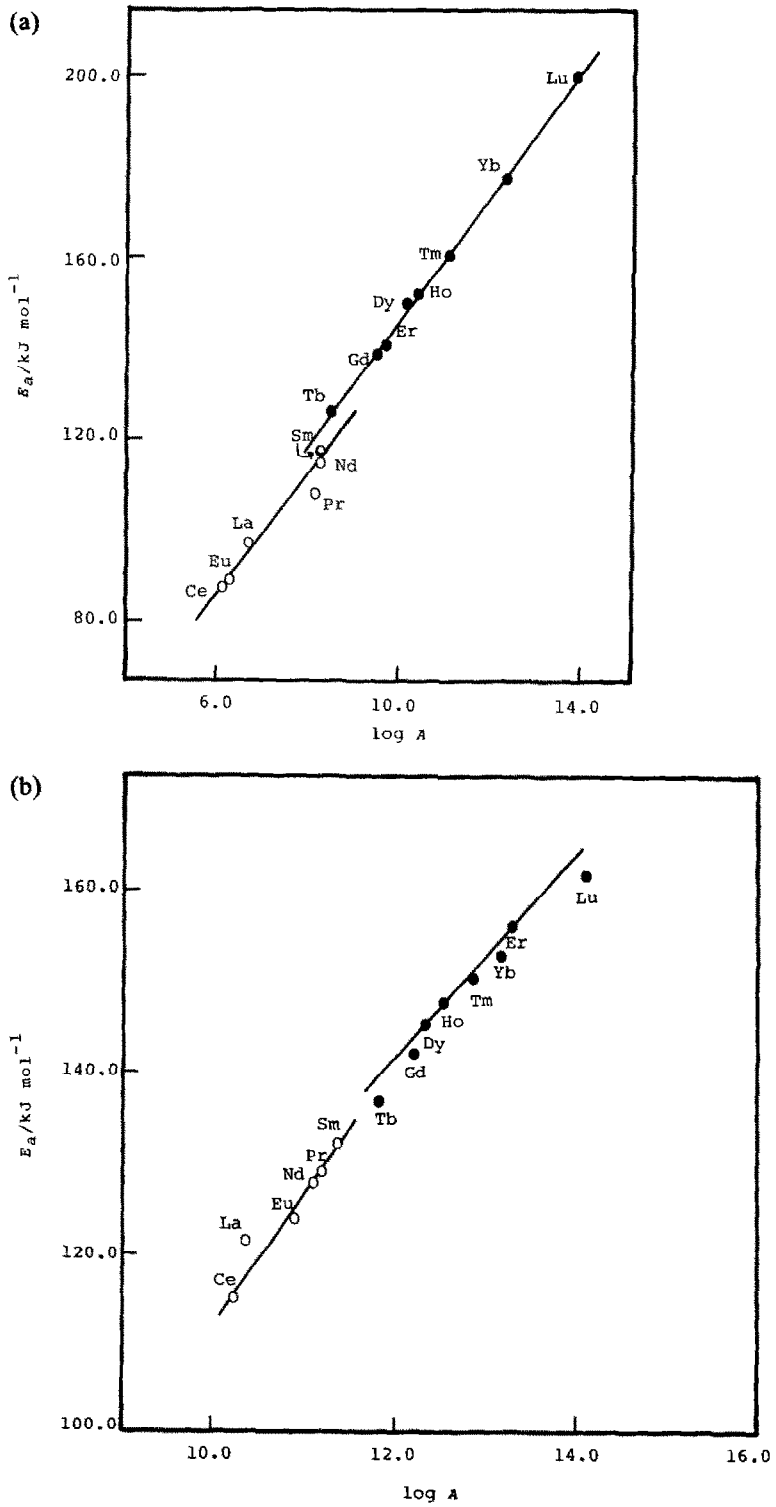

Fig. 4. Kinetic compensation effect in the thermal decomposition of (a) Ln_2ox_3 (b) Ln_2mal_3 and (c) Ln_2suc_3.

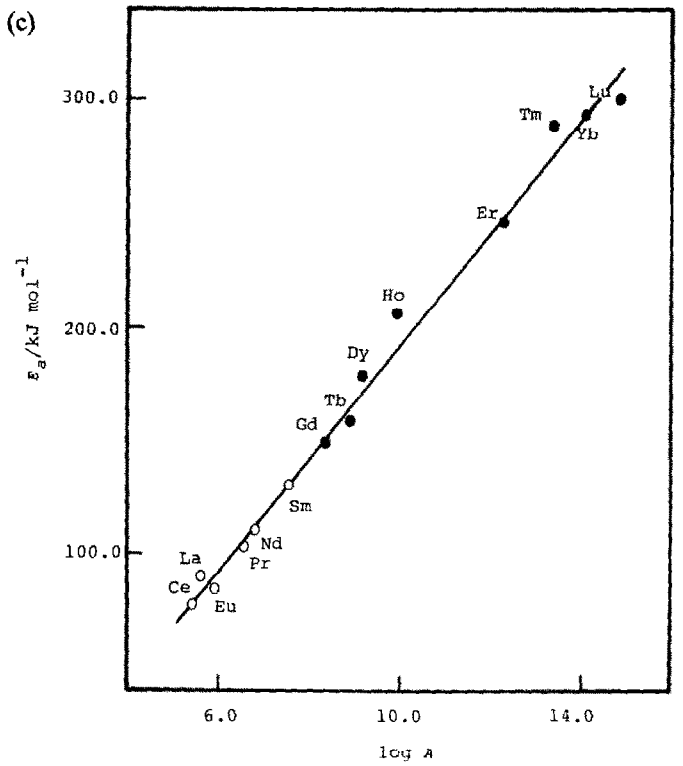

Fig. 4. (continued)

TABLE 2

Kinetic compensation parameters for non-isothermal runs of the thermal dehydration and decomposition of lanthanide dicarboxylates

Compound	Reaction	Ln	*a*	*b*	*γ*
Oxalates					
$Ln_2ox_3 \cdot nH_2O$	Dehydration	L	0.1545	−1.0684	0.9955
		H	0.1356	−1.8458	0.9937
Ln_2ox_3	Decomposition	L	0.0820	−1.1230	0.9833
		H	0.0735	−0.6390	0.9982
Malonates					
$Ln_2mal_3 \cdot nH_2O$	Dehydration	L	0.1022	1.7745	0.9904
		H	0.1159	1.1776	0.9989
Ln_2mal_3	Decomposition	L	0.0740	1.6438	0.9958
		H	0.0932	−0.9983	0.9850
Succinates					
$Ln_2suc_3 \cdot nH_2O$	Dehydration	L	0.1342	1.6620	0.9853
		H	0.1307	2.3129	0.9964
Ln_2suc_3	Decomposition	L–H	0.0396	2.2492	0.9952

Key: L, light lanthanide; H, heavy lanthanide; γ, correlation coefficient of the linear regression analysis of the E_a–lg A plot.

RESULTS AND DISCUSSION

Figure 2 gives the Coats–Redfern plot for the first dehydration step of samarium oxalate decahydrate $Sm_2ox_3 \cdot 10H_2O$ (ox = oxalate) as a typical example. The plot of $[-\lg(1-(1-\alpha)^{1-n}/T^2(1-n)]$ vs. $1/T \times 10^3$ for $n = 2/3$ results in a straight line with a slope of $-E_a/2.303R$. When the reaction order n was assumed to be 2/3, the plots gave a straight line for all the samples, indicating that the reaction begins on the surface of the crystals and then proceeds uniformly to their centres. The plots of the corresponding values of E_a vs. $\lg A$ (Figs. 3 and 4) lead to the compensation effects for the thermal dehydration and decomposition of the three lanthanide dicarboxylate series. The compensation parameters a and b given in Table 2 were determined in terms of eqn. (1). It is noted that the Jaffe correlation coefficients (γ) [31] of the linear regression analysis of E_a–$\lg A$ plots are close to unity, as shown in Table 2. The values of r indicate good linearity between E_a and $\lg A$. Zsako et al. [32] assumed that the value of the parameter a characterizes the strength of the bond being split when gaseous products are formed the stronger the bond that has to be ruptured, the smaller is the coefficient a. The coefficients a and b in eqn. (1) depend solely on the temperature range of the reaction and on the rate constant [33]

$$a = 2.3RT \qquad b = \lg k \tag{6}$$

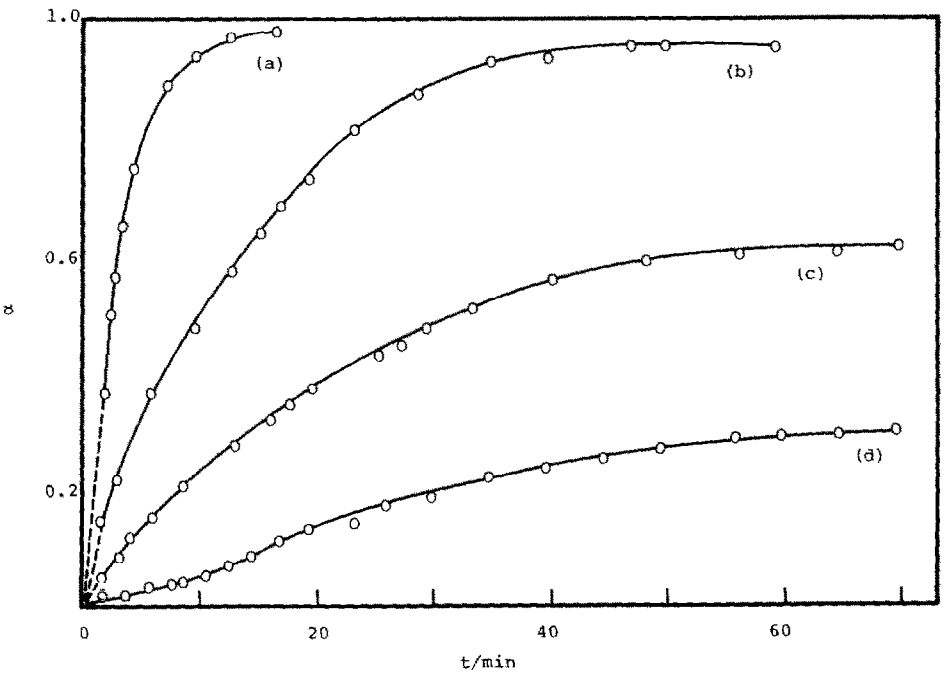

Fig. 5. Isothermal decomposition curves for $Eu_2mal_3 \cdot 6H_2O$ in a flowing N_2 atmosphere. T (K): (a) 443, (b) 413, (c) 398, (d) 388.

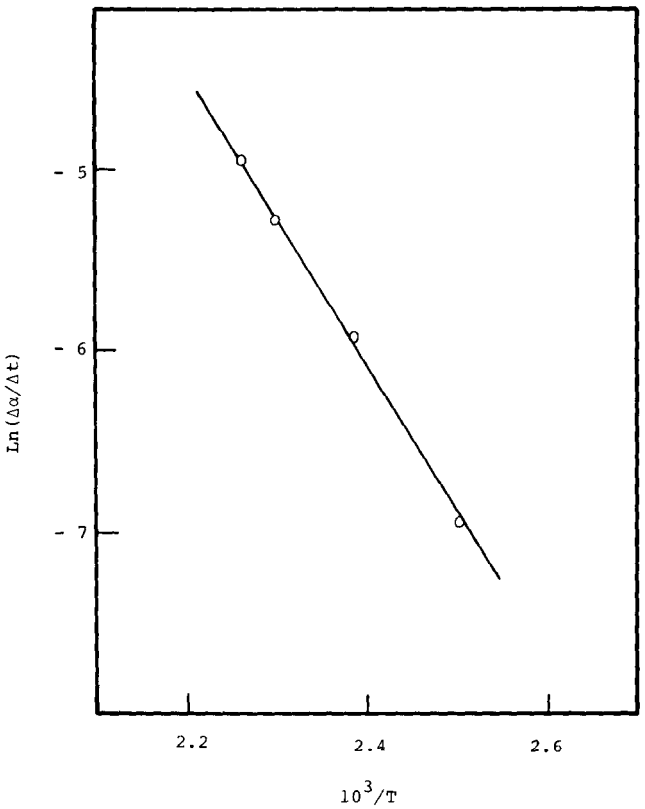

Fig. 6. Plot of $\ln(\Delta\alpha/\Delta t)$ as a function of $1/T$ for the dehydration of $Eu_2mal_3 \cdot 6H_2O$ in a flowing N_2 atmosphere.

A statistical analysis of the data has been carried out by means of the least-squares method to determine the constants *a* and *b*. As shown in Table 2, closeness of the average values of the non-isothermal kinetic parameter *a* was observed for the processes of both the dehydration and the decomposition of the three dicarboxylates. Although there is a slight difference in the compensation coefficient *a* among the three dicarboxylates, the *a* values obtained indicate similar bond strength of the metal leaving group in the three dicarboxylates. The compensation parameter *b* in eqn. (1) is related to the structure of and defects in the starting material or to the mobility of the crystal lattice [34]. Zsako et al. [35] have stated that the parameter *b* includes larger probable errors than the parameter *a*. The *b* values obtained in the present work showed complex tendencies and were difficult to discuss systematically.

The plot of E_a vs. $\lg A$ for the dehydration and decomposition steps of the three dicarboxylates, apart from the decomposition step of the succinates, showed two linear portions for the light and the heavy lanthanides, as shown in Figs. 3 and 4. The representation of two straight

lines reflects the double periodicity between the former half and the latter half of the lanthanide sequence.

Ray [36] and many other researchers have stated that non-isothermal data differ sometimes from data for isothermal experiments. In order to check the non-isothermal data in the first dehydration step of $Eu_2mal_3 \cdot 6H_2O$ (mal = malonate), the Ng method [30] was used under isothermal condition. The relationship of the fractional dehydration a to the reaction time t for the isothermal dehydration of $Eu_2mal_3 \cdot 6H_2O$ is shown in Fig. 5. A plot of the left-hand side of eqn. (5) vs. $1/T$ gave a straight line (Fig. 6) to yield an E_a value of 63.5 kJ mol^{-1}, which agreed approximately with that from the non-isothermal Coats–Redfern method (65.7 kJ mol^{-1}).

If we look at the compensation plots in the dehydration processes of hydrated dicarboxylates a little more closely, the elements of the light and heavy lanthanide malonates and the light lanthanide succinates show a different order for the two dicarboxylates. It can be presumed that this reflects some differences in crystal structure which cause variable retention of contained water. For the decomposition, two straight lines for the light and the heavy lanthanides on the plots of E_a vs. A lie in a similar relationship to one another for the three dicarboxylates, and the various elements lie on the lines in almost the same sequence for the decompositions. Furthermore, the separation between the two straight lines decreases from oxalates to malonates, and the plots for the succinates eventually give a single straight line. This tendency may occur owing to the concealment of the periodic properties of the lanthanides, such as ionic radius, by the bulky malonate and succinate ions with their increasing numbers of CH_2 groups in the carboxylates.

REFERENCES

1 F.H. Constable, Proc. R. Soc. London, Ser. A, 108 (1923) 355.
2 E. Cremer and G.M. Schwab, Z. Phys. Chem., Abt. A, 144 (1929) 243.
3 A.K. Galwey, Adv. Catal., 26 (1977) 247.
4 B.J. McCoy, J. Chem. Phys., 80 (1984) 3629.
5 V.P. Zhdanov, Surf. Sci., 159 (1985) L416.
6 R.K. Agrawal, J. Therm. Anal., 31 (1986) 73.
7 K.J. Laider, Chemical Kinetics, 2nd edn., McGraw-Hill, New York, 1965, p. 251.
8 I. Horvath, Thermochim. Acta, 85 (1985) 193.
9 G.G.T. Guarini, R. Spinicci and L. Virgili, J. Therm. Anal., 13 (1978) 263.
10 D. Dollimore, G.R. Heal and J. Mason, Thermochim. Acta, 24 (1978) 307.
11 P.W.M. Jacobs and W.L. Ng, Reactivity of Solids, Proc. 7th Int. Symp., Chapman and Hall, London, 1972, p. 398.
12 M.R. Alvarez, M.J. Tello and E.H. Bocanegra, Thermochim. Acta, 43 (1981) 115.
13 C. Fairbridge, R.A. Ross and P. Spooner, Wood Sci. Technol., 9 (1975) 257.
14 J.M. Criado and M. Gonzales, Thermochim. Acta, 46 (1981) 201.

15 S.V. Levchik, G.F. Levchik and A.I. Lesnikovich, J. Appl. Polym. Sci., 37 (1989) 1391.
16 P.G. Schullerus, L. Patron, S. Plostinaru, A. Contescu and E. Segal, Thermochim. Acta, 153 (1989) 263.
17 B. Packwska and J. Pysiak, Thermochim. Acta, 167 (1990) 145.
18 R. Larsson, Catal. Today, 1 (1987) 93; Chem. Scr., 27 (1987) 371.
19 W. Linert and V.N. Sapunov, Chem. Phys., 119 (1988) 265.
20 A. Peled, D. Naot and M. Perakh, Colloid Polym. Sci., 266 (1988) 958.
21 G.V. Lewis and C.R.A. Catlow, J. Phys. Chem. Solids, 47 (1986) 89; C.T.J. Peng and H.Y. Lu, J. Am. Ceram. Soc., 71 (1988) C44.
22 P.A. Tanguy, L. Choplin and P. Hurez, Polym. Eng. Sci., 28 (1988) 529.
23 R.K. Agrawal, J. Therm. Anal., 35 (1989) 909.
24 H.M.J. Boots and P.K. de Bokx, J. Phys. Chem., 93 (1989) 8240; P.K. de Bokx and H.M.J. Boots, J. Phys. Chem., 93 (1989) 8243.
25 J. Norwisz, Z. Smieszek and Z. Kolenda, Thermochim. Acta, 156 (1989) 313.
26 (a) K. Nagase, K. Muraishi, K. Sone and N. Tanaka, Bull. Chem. Soc. Jpn., 48 (1975) 3184; K. Muraishi, K. Nagase and N. Tanaka, Thermochim. Acta, 23 (1978) 125; K. Muraishi, T. Takano, K. Nagase and N. Tanaka, J. Inorg. Nucl. Chem., 43 (1981) 2293; K. Muraishi, K. Nagase, M. Kikuchi, K. Sone and N. Tanaka, Bull. Chem. Soc. Jpn., 55 (1982) 1845; K. Muraishi and K. Nagase, Thermochim. Acta, 159 (1990) 225; K. Muraishi, Thermochim. Acta, 164 (1990) 401; K. Nagase, H. Yokobayashi, K. Muraishi and M. Kikuchi, Thermochim. Acta, 177 (1991) 273; K. Muraishi, H. Yokobayashi and K. Nagase, Thermochim. Acta, 182 (1991) 209. (b) K. Nagase, H. Yokobayashi, K. Muraishi and K. Sone, Bull. Chem. Soc. Jpn., 48 (1975) 1612; H. Yokobayashi, K. Nagase and K. Muraishi, Bull. Chem. Soc. Jpn., 48 (1975) 2789.
27 K. Muraishi, K. Nagase, M. Kikuchi, K. Sone and N. Tanaka, Bull. Chem. Soc. Jpn., 55 (1982) 1845.
28 A.W. Coats and J.P. Redfern, Nature, 201 (1964) 68.
29 K.N. Ninan, J. Therm. Anal., 35 (1989) 1267.
30 W.L. Ng, Aust. J. Chem., 28 (1975) 1169.
31 H.H. Jaffe, Chem. Rev., 53 (1953) 191.
32 J. Zsako, Cs. Varhelyi and E. Kekedy, Proc. 4th Int. Conf. Therm. Anal., Budapest, 1974, Vol. 1, Heyden, 1975, p. 177.
33 A.V. Nikolaev and V.A. Logvinenko, J. Therm. Anal., 10 (1976) 363; N. Eisenreich, J. Therm. Anal., 19 (1980) 289.
34 A.I. Lesnikovich and S.V. Levchik, J. Therm. Anal., 30 (1985) 677.
35 J. Zsako, Cs. Varhely, G. Liptay and K. Szilagyi, J. Therm. Anal., 7 (1975) 41.
36 H.S. Ray, J. Therm. Anal., 24 (1982) 35.

APPENDIX

In the Coats–Redfern equation, when $n = 1$ (ICH = 1), $B(I)$ is calculated by the eqn. of the left-hand side *[3.1]* in the flow diagram of Fig. 1 (hereafter referred to as *[3.1]*). $n = 2/3$ (ICH = 2), $B(I)$ in the right-hand side is calculated by $Y(I) = y_i = -\lg[-\lg(1-\alpha)^{1-n}/T^2(1-\alpha)]$ as shown in *[3.2]*. Similarly, $X(I)$ is obtained by $X_i = 1/T$ *[4]*. In this manner there is determined a set of (x_i, y_i) values. The Coats–Redfern equation may thus be expressed mathematically

$$y = ax + b \tag{A1}$$

To determine the most probable values of a and b, calculations by the least-squares method are carried out for reliable data *[5]*. Namely

$$S = \sum_{i=1}^{n} [(ax_i + b) - y_i]^2 \tag{A2}$$

$$\begin{aligned} \frac{\partial S}{\partial a} = 0 \qquad & 2\sum_{i=1}^{n} [(ax_i + b) - y_i]x_i = 0 \\ \frac{\partial S}{\partial b} = 0 \qquad & 2\sum_{i=1}^{n} [(ax_i + b) - y_i]1 = 0 \end{aligned} \tag{A3}$$

From eqns. (A2) and (A3)

$$a\sum_{i=1}^{n} x_i x_i + b\sum_{i=1}^{n} x_i = \sum_{i=1}^{n} y_i x_i \tag{A4}$$

$$a\sum_{i=1}^{n} x_i + b\sum_{i=1}^{n} 1 = \sum_{i=1}^{n} y_i \tag{A5}$$

therefore

$$\begin{pmatrix} \Sigma x_i x_i & \Sigma x_i \\ \Sigma x_i & 1 \end{pmatrix}\begin{pmatrix} a \\ b \end{pmatrix} = \begin{pmatrix} \Sigma y_i x_i \\ \Sigma y_i \end{pmatrix} \tag{A6}$$

Multiplying both sides of eqn. (A6) by the inverse matrix $\begin{pmatrix} \Sigma x_i y_i & \Sigma x_i \\ \Sigma x_i & \Sigma 1 \end{pmatrix}^{-1}$ gives

$$\begin{aligned} \begin{pmatrix} a \\ b \end{pmatrix} &= \begin{pmatrix} \Sigma x_i y_i & \Sigma x_i \\ \Sigma x_i & \Sigma 1 \end{pmatrix}^{-1}\begin{pmatrix} \Sigma y_i x_i \\ \Sigma y_i \end{pmatrix} \\ &= \frac{1}{\begin{vmatrix} \Sigma x_i y_i & \Sigma x_i \\ \Sigma x_i & \Sigma 1 \end{vmatrix}}\begin{pmatrix} \Sigma 1 & \Sigma x_i \\ \Sigma x_i & \Sigma x_i x_i \end{pmatrix}\begin{pmatrix} \Sigma y_i x_i \\ \Sigma y_i \end{pmatrix} \end{aligned} \tag{A7}$$

Based on the relationship described above, values were obtained for the activation energy and frequency factor A(FF(ICH)) *[6]*. When $n = 2/3$ the linearity of the Coats–Redfern plot has been found to be entirely satisfactory.